RANKING OF FUEL–AIR MIXTURES IN TERMS OF THEIR PROPENSITY TO DEFLAGRATION-TO-DETONATION TRANSITION

S. M. Frolov[1,2,3], **V. I. Zvegintsev**[4], **V. S. Aksenov**[1,2], **I. V. Bilera**[5], **M. V. Kazachenko**[1,6], **I. O. Shamshin**[1,3], **P. A. Gusev**[1,7], **and M. S. Belotserkovskaya**[3,8]

[1]N. N. Semenov Federal Research Center for Chemical Physics of the Russian Academy of Sciences
4 Kosygin Str., Moscow 119991, Russian Federation
[2]National Research Nuclear University MEPhI (Moscow Engineering Physics Institute)
31 Kashirskoe Sh., Moscow 115409, Russian Federation
[3]Federal State Institution "Scientific Research Institute for System Analysis of the Russian Academy of Sciences"
36-1 Nakhimovskii Prosp., Moscow 117218, Russian Federation
[4]S. A. Khristianovich Institute of Theoretical and Applied Mechanics Siberian Branch of the Russian Academy of Sciences
4/1 Institutskaya Str., Novosibirsk 630090, Russian Federation
[5]A. V. Topchiev Institute of Petrochemical Synthesis Russian Academy of Sciences
29 Leninsky Prosp., Moscow 119991, Russian Federation
[6]N. E. Bauman Moscow State Technical University
5-1 Baumanskaya 2nd Str., Moscow 105005, Russian Federation
[7]Joint Institute for High Temperatures Russian Academy of Sciences
13-2 Izhorskaya Str., Moscow 125412, Russian Federation
[8]Institute for Computer Aided Design Russian Academy of Sciences
19/18 Brestskaya 2nd Str., Moscow 123056, Russian Federation

A new experimental method for evaluating the detonability of fuel–air mixtures (FAMs) based on measuring the deflagration-to-detonation

DOI: 10.30826/ICPCD12B02

transition (DDT) run-up distance and/or time in a standard pulse detonation tube (SDT) is used to rank gaseous premixed and non-premixed FAMs by their detonability under substantially identical thermodynamic and gasdynamic conditions. In the experiments, FAMs based on hydrogen, acetylene, ethylene, propylene, propane–butane, *n*-pentane, and natural gas (NG) of various compositions as well as FAMs based on the gaseous pyrolysis products of polyethylene (PE) and polypropylene (PP) are used: from extremely fuel-lean to extremely fuel-rich at normal temperatures and pressures. The concept of "equivalent" FAMs exhibiting the same or similar detonability under the same conditions is proposed. "Equivalent" FAMs can be used for predictive physical modeling of detonation processes involving FAMs of other fuels. The ranking of FAMs in terms of their relative detonability allows choosing a propylene FAM for physical modeling of the operation process in the PP-fueled solid-fuel ramjets operating on detonative combustion.

1 Introduction

The term "detonability" with respect to FAMs implies the ability of a reactive mixture of a given composition to support the propagation of a stationary detonation wave in various thermodynamic (e. g., in terms of pressure and temperature) and gasdynamic (e. g., in terms of the level of turbulence) conditions. The detonability of FAMs, on the one hand, determines their explosion hazards during storage, transportation, and use in various sectors of the economy and, on the other hand, the possibility of their practical application in advanced energy-converting devices operating on detonative combustion [1].

The detonability of reactive mixtures is a relative concept. As a method for its evaluation, one can take a comparison of the mean cell size of multifront detonation propagating in a premixed FAM of a particular fuel under normal conditions with the cell size of any selected (reference) FAM, for example, stoichiometric composition under the same conditions [2]. In this case, the mean size of the detonation cell in the reference FAM is taken as a measure of detonability and the detonability of all other FAMs is estimated with respect to this measure: the larger the cell size, the lower the detonability.

As a method for estimating FAM detonability, one can also compare the critical energy of direct initiation of spherical detonation in a quiescent premixed FAM under normal conditions with the critical energy of direct initiation of spherical detonation of any selected (reference) FAM, for example, stoichiometric composition under the same conditions [2]. In this case, the critical energy of the direct initiation of spherical detonation in the reference FAM is taken as a detonability measure and the detonability of all other FAMs is estimated with respect to this measure: the higher the direct initiation energy, the lower the detonability.

Other methods and measures for assessing the relative detonability of a given FAM include the comparison of FAMs by the critical diameter of detonation transmission from a tube to an unconfined volume [2] and/or by the limiting diameter of detonation propagation in a straight tube with smooth walls [3]. In addition, the methods and measures for assessing the relative detonability can include the comparison of FAMs by the run-up distance of the DDT, first proposed by Sokolik and Shchelkin [4–6]. To complete the picture, one should also mention methods for evaluating the detonability of motor fuels for internal combustion engines, described in detail in national and international standards. In some of them, the composition of the reference fuel is determined which is a mixture of isooctane and n-heptane detonating under the same conditions as the test motor fuel. In the others, the relative detonability of motor fuel is evaluated at the maximum power of a single-cylinder engine operating under certain conditions. In both cases, the Octane Number is used as a measure of relative detonability which is numerically equal to the volumetric content of isooctane in the reference fuel.

It is worth noting that all of the above methods and measures for evaluating the detonability of FAMs are based solely on the experiment: the current level of development of the detonation theory does not yet allow reliable assessment of the detonability of FAMs in different conditions based on unambiguous scientifically grounded criteria. The experimental determination of the detonation cell size, the energy of direct initiation of spherical detonation, the critical diameter of the transmission of detonation from the tube into an unconfined volume, and/or the limiting diameter of the propagation of detonation in a straight tube with smooth walls, even for gaseous

FAMs, is accompanied with great difficulties and large measurement errors. The difficulties are caused by the need in using strong sources of initiation (charges of high explosives weighing up to 100 g and above, powerful electric discharges, etc.), detonation tubes of various dimensions, etc. Large measurement errors are caused by the substantially nonuniform cellular structure of multifront detonation of gaseous FAMs (for the same FAM under the same conditions, the cell size can vary several times) and the critical nature of the phenomena of initiation of spherical detonation, transmission of detonation from the tube into the unconfined volume, and propagation of detonation in smooth tubes of near-limiting diameter. It is even more difficult to evaluate the detonability of two-phase FAMs containing liquid or solid fuel in the form of fine droplets or particles: the cellular structure of detonation in two-phase FAMs is observed only at very small droplet and particle sizes (at a level of 10 μm or less) [7], and the critical initiation energy of spherical detonation depends on the content of the vapor phase in a two-phase FAM, i. e., depends on the time delay between the creation of the FAM cloud and the initiation of detonation. If one adds the dependence of mixture detonability on the thermodynamic conditions (pressure and temperature different from their normal values) as well as on the gasdynamic conditions (nonzero velocity of the FAM flow, turbulence, heterogeneity of the composition of the FAM, etc.), then a comprehensive solution to the problem of estimating mixture detonability based on the above methods and measures seems unrealistic.

To follow the ideas of [4–6], we propose herein an alternative method for estimating the detonability of FAMs based on measuring not only the DDT run-up distance, but also the DDT run-up time in an SDT under substantially identical thermodynamic and gasdynamic conditions. This method is applicable to both gaseous and two-phase FAMs based on liquid and solid fuels. The objective of this work is to develop the experimental technique for simple and reliable estimation of the comparative detonability of FAMs.

2 Test Bench

Figure 1 shows the schematic of a test bench with the SDT. This test bench is essentially the modernized detonation tube used in our ear-

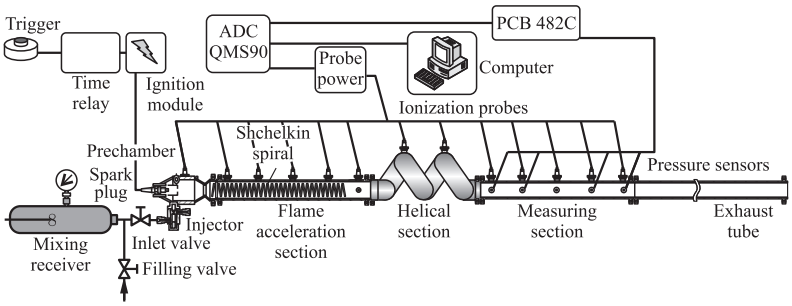

Figure 1 Schematic of the test bench with the SDT

lier studies related to the liquid-fueled pulsed detonation engine [8]. The geometry of the tube and ignition arrangement were thoroughly optimized in [8] for obtaining the shortest possible DDT run-up distance.

The main element of the bench is an open-type pulse-detonation tube, which includes a prechamber and three sections: a flame acceleration section with a Shchelkin spiral, a helical section of the tube for gasdynamic focusing of a shock wave, and a measuring section, a straight and smooth section for measuring pressure in the propagating detonation wave and the velocity of detonation [9, 10]. The bench includes control units, ignition and registration systems, and measuring probes.

The FAM can be prepared in a mixing receiver which is connected through a filling valve to a comb (not shown in Fig. 1). Through the comb, the mixing receiver is connected to a vacuum pump, an air compressor, and to a cylinder with combustible gas. Premixed FAM through the inlet valve is fed to the injector from which the mixture enters the prechamber of the SDT.

Fuel components can be also supplied separately to the SDT. In this case, air is forced by the blower or comes under pressure from an air receiver to the prechamber, whereas gaseous/liquid fuel is supplied in the form of a jet/spray into it. If the fuel is represented by the gasification/pyrolysis products of solid fuel, then it is supplied under pressure from the gas generator (GG).

The FAM in the SDT is ignited by a car spark plug installed in the prechamber. A high voltage is supplied to the spark plug from the ignition module. The control signal turning on the ignition module is supplied from the time relay (Temp-1M). Two ignition arrangements are used: standard spark ignition and pulsed jet ignition. In the main series of experiments, the pulsed jet ignition is applied. The spark ignition is used in a limited number of experiments.

The arrangement of the pulsed jet ignition is as follows. The spark plug is placed in a hollow cylinder 30 mm in diameter and 33 mm long. At the top wall of the cylinder, there is a central hole 8 mm in diameter. At the lateral wall of the cylinder, there are two belts of venting holes 5 mm in diameter: one belt of 3 equidistant holes and another belt of 3 equidistant holes rotated by 60° around the cylinder axis. The pulsed jet ignition method has been known for a long time [11, 12]. It is used to significantly increase the flame velocity at the initial stage of flame propagation as compared to the standard spark ignition.

After ignition, the flame from the prechamber enters the flame acceleration section in which the Shchelkin spiral is installed. At the near end, the spiral is fixed with a bolt. Along the length, the spiral is additionally fixed with protruding ionization probes (IPs) which do not allow large deformations of the spiral during the experiment. Two spirals are used in the experiments. Table 1 lists spiral parameters: length L, wire diameter s, outer diameter d, number of turns n, pitch h, and blockage ratio BR calculated by the formula:

$$\mathrm{BR} = \frac{4s(d-s)}{d_a^2}$$

where d_a is the inner diameter of the flame acceleration section. In the main series of experiments, Spiral 1 with BR = 0.46 is used. Spiral 2 with BR = 0.24 is used in a limited number of experiments.

Table 1 Parameters of spirals used in experiments

Spiral	L, mm	s, mm	d, mm	n	h, mm	BR
1	930	6.7	50	38	22–26	0.46
2	940	6.7	29	40	21–24	0.24

The helical section of the SDT is intended for gasdynamic focusing of compression waves and reflections of shock waves stimulating localized self-ignition centers to occur in the flow, which ultimately leads to detonation onset by the mechanism [13]. The helical section is a tube twisted into a spiral with short straight sections of 50 mm in length from both ends of the section. The outer diameter of the helical section is 136 mm, the inner is 36 mm, and the pitch is 220 mm. The parameters of the detonation wave (its amplitude and velocity) are measured in the measuring section of the SDT. The inner diameter of the tube in all three sections is 50 mm. The overall length of the first, second, and third sections is 1060, 908, and 1060 mm, respectively. The length and inner diameter of the prechamber are 200 and 70 mm. An additional smooth section with a length of 1790 mm is attached to the end of the third section: an exhaust tube forwarding the detonation products to the ventilation shaft. The total path length of the SDT is 5040 mm.

Figure 2 shows a schematic of the SDT indicating the numbers of the measuring cross sections (the locations of IPs and pressure sensors (PSs)) and the distances between them. In total, 13 measuring sections are located along the tube. In sections **0**–**7** and **10**, only IPs are installed and in sections **8**, **9**, **11**, and **12**, IPs and PSs are installed. The distances between the sensors in the measuring sections are as follows: **0**–**1** — 270 ± 1 mm; **1**–**5** and **8**–**12** — 240 ± 1 mm. The distance between sections **5** and **6** as well as **7** and **8** is also equal to 240 ± 1 mm and between sections **6** and **7**, it is 220 ± 1 mm.

When calculating the average velocity of a pressure wave in the helical section, it is necessary to know the distance traveled by the

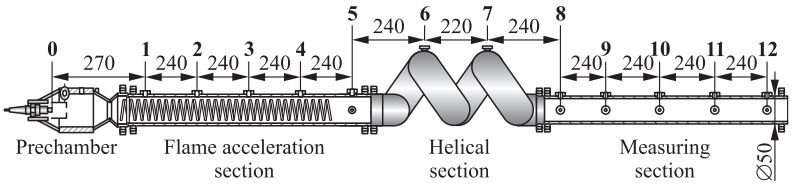

Figure 2 Schematic of the SDT with the indication of measuring segments: **0** — ignition point; and **1**–**12** — sections with IPs and/or PSs. Dimensions are in millimeters

wave. The base distances here are the distances between control points measured along the outer surface of the helical section which are taken to be 300 ± 5 mm for the distance between points **5** and **6**, 370 ± 5 mm for the measuring segment **6**–**7**, and 315 ± 5 mm for a measuring segment **7**–**8**.

3 Methodology for Conducting Tests with Premixed Gases

When the tests are conducted with premixed FAMs, the FAMs are prepared in the mixing receiver (see Fig. 1) with a volume of 40 l by partial pressures. The components of the FAMs are mixed with a fan for at least 10 min. The repeatability error in setting the partial pressure of the component with the lowest concentration (fuel) does not exceed 0.1 kPa (1%). The pressure is monitored by the absolute pressure Courant-DA (600 kPa) sensor with an accuracy class of 0.15. The absolute error of the pressure measurement is 1 kPa. An additional error in the measurement of the partial air pressure is introduced by the uncertainty in the gas temperature in the mixer and this additional error is estimated as 1.0%–1.5%. The maximum error in determining the fuel–air equivalence ratio is estimated as 1.5%. The volume of the prepared mixture is sufficient for 5–6 tests.

When filled with the FAM, the SDT is blown with at least 4 times the volume of the FAM relative to the volume of the detonation tube equal to $\sim$ 5 l. The volume of the blown FAM (at least 20 l) is controlled by the pressure drop in the mixing receiver: the pressure drop during purging is at least 50 kPa.

The instantaneous location of the flame is determined using IPs. The principle of their action and the measurement procedure are described in [14]. The maximum measured ionization current (short circuit current) is 0.5 mA. The IP is a central axial electrode in the insulator pressed into a threaded steel sleeve like a standard car spark plug. The length of the central electrode protruding from the sleeve into the SDT is 25 mm. Ionization probes are installed in each of 12 measuring sections. The accuracy of determining the location of the flame using IPs is ± 2 mm.

To register the amplitude and profile of pressure in the detonation wave, PCB 113B24 high-frequency piezoelectric PSs with a natural frequency of 500 kHz are used. The PSs are installed on the SDT through special electrovibration-insulating sleeves to reduce the effects of electrical interference and elastic waves propagating along the metal wall of the tube. In a smooth tube in sections **8**, **9**, **11**, and **12**, four PSs are installed (see Fig. 2). The accuracy of determining the location of a pressure wave using high-frequency PSs is ±6 mm.

The experiments are performed according to the following procedure. The tube is blown with air from the compressor for 1–2 min with an average air flow rate of about 1 l/s. Then, the tube is blown through with the FAM from the mixing receiver until the volume of the FAM equal to 4 times the volume of the SDT passes through the tube. The FAM volume is controlled by the pressure drop in the mixing receiver and the flow rate is controlled by the inlet valve so that the pressure decreases at a rate of 0.5–1 kPa/s. After closing the inlet valve and starting the analog-to-digital converter (ADC), the time relay triggers the ignition command: a pulse of a 10-millisecond duration to the ignition module and the mixture is ignited by the spark plug. After saving the waveform in the memory of computer, the experiment is repeated a specified number of times ("shots"). The number of shots for each mixture of a certain composition, as a rule, varies from 3 to 8 and increases with approaching the limiting conditions of DDT. According to the records of PSs and IPs, the velocities of the leading shock wave (PSs) and combustion waves (IPs) are calculated and the "distance–time" diagrams and "wave velocity – distance" diagrams of the process development are plotted. Time is measured with the accuracy determined by the ADC sampling frequency (375 kHz). For the worst case (a short measuring segment of 240 mm and a wave velocity of 2000 m/s), the relative error in determining the wave velocity does not exceed 3%.

The detonability of FAMs of different fuels and different compositions is estimated by the DDT run-up distance L_{DDT} and/or run-up time t_{DDT} provided that the propagation of self-sustaining detonation is recorded in the measuring section of the SDT. Self-sustaining detonation is understood to mean a stationary propagating super-

sonic explosion process, the speed of which at the last two measuring segments in the measuring section of the SDT is constant with an accuracy of ±3% and the fronts of the leading shock wave and the combustion wave match within ±6 μs. Particular attention is paid to reproducibility of the results: a detonation wave is considered stationary if, in all experiments with a FAM of a given composition, it propagates at the same supersonic speed. A similar approach to the identification of detonation was previously used in [15].

4 Methodology for Conducting Tests with Nonpremixed Gases

For investigating the detonability of nonpremixed gaseous compositions, the SDT is equipped with the flow mixer. The flow mixer is a cylindrical channel with a converging-diverging (C-D) nozzle. Air is supplied through the air inlet fitting to the air channel 6 mm in diameter via the annular air plenum with 9 connecting holes 2 mm in diameter. From the air channel, air passes through the C-D nozzle with a critical section 2 mm in diameter. Combustible gas is supplied from a cylinder through the fuel inlet fitting to the fuel plenum and then is injected into the diverging part of the C-D nozzle through three calibrated holes 0.7 mm in diameter. The outlet diameter of the mixing channel is 8 mm.

For investigating the detonability of the gasification/pyrolysis products of various solid combustible materials (SCMs) like paraffins, PE, PP, polystyrene, polymethyl methacrylate (PMMA), etc., the SDT is equipped with a special GG in which gasification/pyrolysis of SCMs takes place. The interest in the detonability of such gasification/pyrolysis products originates from the perspective of using SCMs in solid-fuel ramjets operating on detonation [16]. In this study, pellets of PE and PP are used as an SCM. Thermal decomposition of PE and PP occurs in a GG. Figure 3 shows a schematic and a photograph of the GG. The GG consists of a cylindrical casing made of stainless steel. The outer diameter and wall thickness of the casing are 60 and 2.5 mm, respectively.

The height of the casing is 280 mm. A heat accumulator weighing 1 kg is installed inside the casing. The heat accumulator is a mas-

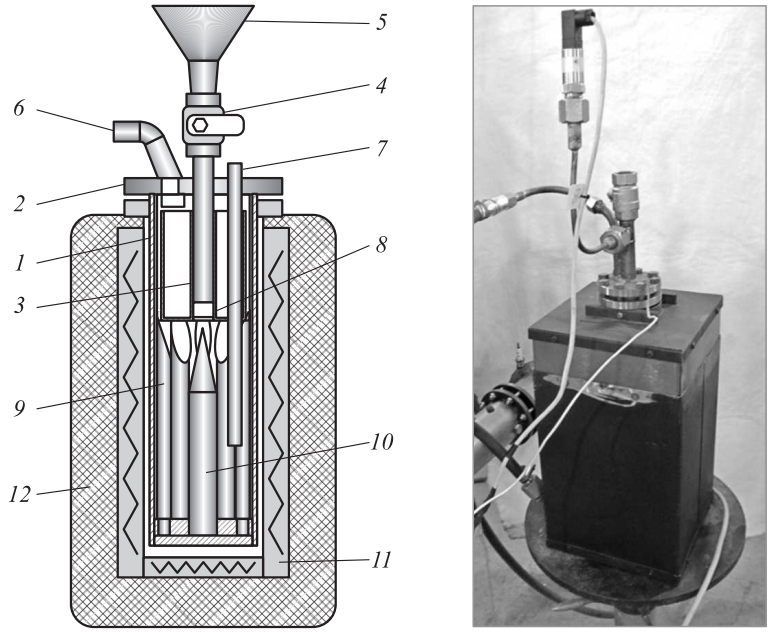

Figure 3 Gas generator: (*a*) schematic (*1* — casing; *2* — removable cover; *3* — pellet feed tube; *4* — ball valve; *5* — pellet loading hopper; *6* — outlet tube for gaseous pyrolysis products; *7* — thermowell of thermoelectric converter; *8* — protective grill; *9* — metal rods; *10* — metal divider; *11* — muffle furnace; and *12* — thermal insulation); and (*b*) photograph

sive metal base on which 10 metal rods and a divider are installed that serve to accumulate heat and to increase the contact area between the heated surface and pellets of solid fuel. When filling, the pellets fall into a figured gap between the divider and the rods. The height of the metal rods is 140 mm. The width of the annular gap between the rods and the divider is 6 mm. The GG casing is closed by a removable cover on which a ball valve with a loading hopper is installed. The passage section of the ball valve is 20 mm. This is enough to quickly load a sample weighing ~ 15 g from pellets of solid fuel with a diameter of 5 mm. When loading, pellets fall into the feed

tube which directs the pellets on the divider. To prevent accidental ingress of large solid pellets into the outlet tube, a protective grill is installed on top of the heat accumulator made in the form of a disk with perforated holes 4 mm in diameter.

Gaseous pyrolysis products are taken from the GG through the outlet tube which is connected to the fuel inlet fitting of the flow mixer. The GG is placed in a muffle furnace, the temperature of which is determined by the preset decomposition temperature T_d in the GG. The decomposition temperature T_d is measured by a Type K thermocouple which is installed inside the protective thermowell (see Fig. 3). The temperature is maintained at a given level by the TPM148 PID-controller (see Fig. 1) with an accuracy of ± 5 °C.

The characteristics of the GG are determined in preliminary tests at T_d ranging from 650 to 850 °C. In these tests, the gaseous pyrolysis products expel from the GG through the nozzle of the flow mixer with air supply turned off. The maximum absolute pressure of the gas in the GG depends on the decomposition temperature increasing with T_d from 0.11 MPa at 650 °C to 0.16 MPa at 800 °C. With an increase in the decomposition temperature, the characteristic time of pressure rise decreases from 20 to 10 s and the total decomposition time decreases from 100 to 80 s. The characteristic time for maintaining pressure at a constant level (within 80% of the maximum pressure) is from 40% to 50% of the total decomposition time.

As an example, Table 2 presents the results of chromatographic analysis of the composition of the gaseous pyrolysis products of PP with the indication of the mass content of the main products in the gas phase for several values of T_d. For products with 4 (C_4) and 5 (C_5)

Table 2 Composition of PP pyrolysis products (%(mass.))

No.	T_d, °C	C_3H_6	*iso*-C_4H_8 (C_4)	C_2H_6	CH_4	C_2H_4	C_3H_8	2-Me-Buten-1 (C_5)	H_2	Rest
1	650	38.8	14.1 (3.2)	12.1	10.2	9.7	3.8	1.2 (3.9)	0.3	9.8 (2.7)
2	650	40.8	14.5 (3.5)	10.7	7.9	8.2	3.8	1.5 (5.3)	0.1	12.5 (3.7)
3	800	27.7	10.7 (4.1)	10.1	21.3	17.7	2.6	0.3 (1.8)	2.0	7.7 (1.7)
4	800	30.4	11.2 (4.0)	10.2	19.4	16.8	2.8	0.6 (1.9)	1.9	6.7 (0.8)

carbon atoms, the numbers in parentheses are the total values of the concentration of products except for isobutene and 2-methylbutene-1. The relative accuracy of determining the composition of the products is ±5%. The analysis shows that the gaseous products mainly consist of propylene, isobutene, ethane, methane, ethylene, and propane. At the highest decomposition temperature (800 °C), the content of hydrogen is also getting large (~ 2 %(wt.)).

Upon completion of the decomposition of a solid fuel sample, a solid residue is accumulated in the GG. In three trials with a decomposition temperature of 650 °C performed with the identical weighed portions of PP, the average value of the relative mass of the solid residue is 4.9%. Ash color is light gray and the primary component is limestone. In three tests with a decomposition temperature of 700 °C, also performed with the identical weighed portions of PP, the average value of the relative mass of the solid residue is 7.3%. When tested with a decomposition temperature of 800 °C, the average relative mass of the solid residue over the results of three tests amounted to 18%. At temperatures of 700 and 800 °C, the main component of the solid residue is soot and the color of the residue is black.

During the test, the temperature of the C-D nozzle in the flow mixer does not exceed 80 °C. After the experiments, deposits of Vaseline type are observed in the fuel plenum in an amount of less than 0.1% of the initial sample weight. Upon discharge into the atmosphere, the pyrolysis products are a thick white smoke that burns in a bright, slightly smoky flame.

In the pyrolysis of synthetic polymers, three types of main products are usually formed: coke residue, noncondensable gases and condensable gases (liquid fraction). In individual tests, hot pyrolysis products are sent from the GG to the refrigerator, a copper coil placed in ice water. The condensed pyrolysis products thus obtained appear as an oily yellow-brown liquid with a characteristic odor. At a decomposition temperature of 700 °C, as a result of pyrolysis of a PP sample weighing $\sim$ 15 g, about 6 ml of a liquid with a density of 0.76 ± 0.02 g/cm^3 is obtained.

The pyrolysis process is a complex of sequential and parallel transformations proceeding simultaneously. The reactions occurring during pyrolysis can be divided into primary reactions with a polymer chain breaking with the formation of a free radical and a double bond

and secondary reactions in which primary decomposition products interact with each other. Chromatographic and mass-spectrometric analysis of the liquid fraction of the PP pyrolysis products shows that the main products are unsaturated branched hydrocarbons (alkenes and dienes) C_8–C_{28} which are formed as a result of primary reactions. Their content in the liquid fraction is 78.6%. Besides, groups of compounds formed as a result of secondary cyclization and condensation reactions are identified: cyclodienes (1.9%), cycloalkenes (1.4%), alkylbenzenes (15.2%), and polycyclic aromatic hydrocarbons (1.1%).

When the tests are conducted with nonpremixed FAMs based on the pyrolysis products of PE and PP, the following procedure is used. First, the cyclogram of the test bench operation is set by programming the time relay. The setting of the duty cycle is based on the fact that the fuel gas is fed into the SDT continuously, whereas the supply of air is portioned. Thus, after starting the timer, the air supply should turn on for 6 s and after this time, a spark plug should be triggered. The duration of air supply depends on its flow rate so that the volume of gases supplied to the SDT is greater than the SDT volume. After ignition, the air supply is briefly (within 0.5 s) blocked and then renewed again. This interruption in air supply is required for providing a plug of the pyrolysis products between the new portion of the fresh FAM and the combustion products of the previous cycle. Thereafter, the cycle with air supply, ignition, and interruption in air supply is repeated a specified number of times ("shots").

A charge of ~ 15 g PE/PP pellets is being prepared. The air receiver of the test bench is filled with air to a predetermined pressure, and the GG is heated to the preset temperature. Next, a sample of pellets is poured into the GG and the ball valve is closed. Thereafter, the command is given to start the ADC and turn on the time relay. Next, the installation works offline until full fuel consumption in successive shots. For example, at an initial temperature of the GG of 700 °C and a charge weight of 15 g, the combustible gas is generated during approximately 60 s. During this time, the SDT produces up to 10 shots.

The solid curve in Fig. 4 shows a typical time history of the absolute gas pressure in a GG loaded with PP sample in one of the tests with 12 shots. For comparison, a dotted curve is obtained under

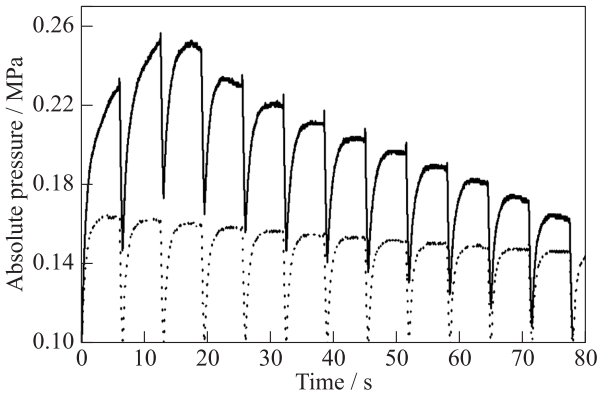

Figure 4 Typical measured time histories of the absolute pressure in the GG in two tests with 12 shots: in the test with PP sample (solid curve) and in the test without PP sample (dotted curve)

the same conditions but without loading PP in the GG. Countdown of time starts from the instant when the pressure starts rising. Sharp dips on the curves are caused by pressure drop in the SDT and in the flow mixer during short stops of the air supply after the shot. In each shot, before the pressure dips, the pressure levels out on the solid curve, thus indicating the stabilization of the process: the rate of gas formation is approximately equal to the rate of gas outflow from the GG. In addition, in some shots on the solid curve, there are sharp peaks before pressure dips. These peaks correspond to shots with DDT. Such shots are conditionally called as *detonative shots*, since they are accompanied by the formation of retonation waves traveling upstream along the SDT and penetrating the manifolds connected to the SDT. The first and second shots on the solid curves are seen to be detonative shots. In the third shot, there is no sharp pressure peak. Shots without sharp pressure peaks are conditionally called as *dry shots*: in such shots, a combustible mixture is either not ignited by a spark plug or, if ignited, the resultant flame is not accelerated to DDT. Further on, the fourth to ninth shots in Fig. 4 are seen to be detonative shots, whereas the shots from tenth to twelfth to be dry shots.

5 Processing of Results: Deflagration-to-Detonation Transition Run-Up Distance and Time

Let us describe the methodology for processing the results of tests using a premixed stoichiometric hydrogen–air mixture and the SDT with Spiral 1 as an example. Figure 5 shows the primary records of IPs (dotted curves) and PSs (solid curves) for one of six successive shots with the FAM of the same composition. The countdown of time starts from the instant of electrical breakdown in the discharge gap of the spark plug. The duration of the electric discharge is 2–2.5 ms. The time instants of a sharp deviation of the records of IPs down from the zero line are treated as the instants of the arrival of the combustion wave in the corresponding measuring section. Similarly, the time instants of a sharp deviation of the records of PSs upward from the zero line are treated as the instants of arrival of a pressure wave or a shock wave in the corresponding measuring section. Knowing the distances of all measuring sections from the ignition source, based on

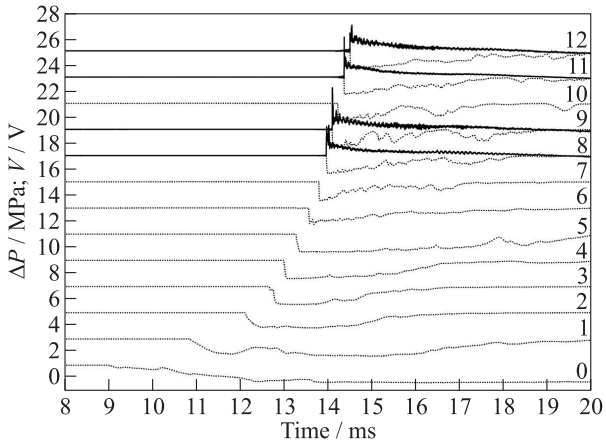

Figure 5 Primary records of IPs (voltage in volts) in sections **0**–**12** (dashed curves) and PSs (overpressure in megapascals) in sections **8**, **9**, **11**, and **12** (solid curves) in a test with stoichiometric hydrogen–air mixture

Fig. 5, it is possible to plot the dependences of the distances traveled by the combustion and pressure waves on time, that is, the distance–time diagram. An example of distance–time diagrams plotted based on the records of IPs and PSs for six successive tests with the same FAM as in Fig. 5 is presented in Fig. 6*a*. Figure 6*b* presents the corresponding wave velocity – distance diagrams.

In Fig. 6*b*, the velocity of the combustion wave, D_f, at each measuring segment is determined by the known distance between the measuring sections in which the IPs are located and by the time interval between the time instants of the arrival of the combustion wave at these IPs. The pressure wave velocity, D_{sw}, is determined in a similar way but instead of the IP records, the PS records are used. The horizontal dashed line in Fig. 6*b* corresponds to the thermodynamic Chapman–Jouguet detonation velocity for a stoichiometric hydrogen–air mixture ($D_{\mathrm{CJ}} \approx 1967$ m/s). Joint consideration of Figs. 6*a* and 6*b* makes it possible to determine the DDT run-up distance and time, L_{DDT} and t_{DDT}, and, therefore, to obtain data for estimating the detonability of a stoichiometric hydrogen–air mixture under normal initial conditions.

The data in Fig. 6 illustrate high repeatability of the results in different SDT shots for a FAM with high reactivity. The data of each shot with a FAM of a certain composition are averaged. Thus, in Fig. 6*b*, the following averaged values are obtained for 6 successive shots: $D_{\mathrm{sw}} = 1958$ m/s and $D_f = 1971$ m/s. The absolute errors in determining these values are only 7 and 12 m/s, respectively. Considering a relative measurement error of 3%, the maximum absolute error of the measured wave propagation velocity is about 60 m/s.

It follows from Fig. 6*b* that the velocity of the combustion wave, D_f, reaches the value D_{CJ} ($D_f \approx D_{\mathrm{CJ}}$) between the measuring sections 7 and 8, i. e., in the shots under consideration DDT occurs close to the exit from the helical section of the SDT. As a matter of fact, after the transition of the combustion wave to the measuring section of the SDT, the time instants of arrival of the combustion wave to IPs in sections **9**, **10**, **11**, and **12** match with the time instants of arrival of the pressure wave to PSs installed in the same sections. This means that a "shock wave – reaction front" complex is formed which propagates at a constant (supersonic) average velocity $D = D_{\mathrm{sw}} \approx D_f$ close to D_{CJ}, that is, the self-sustaining detonation is registered. There-

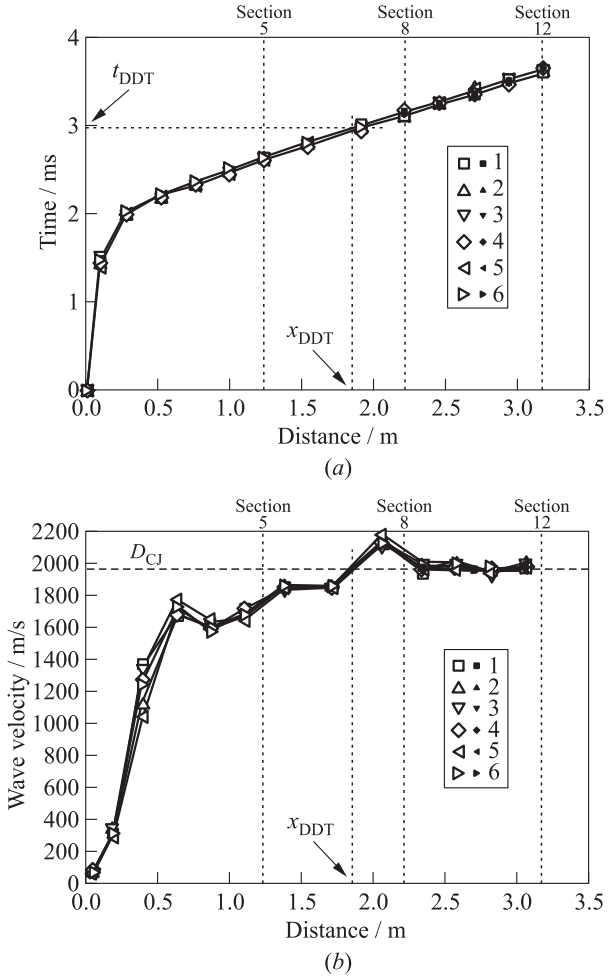

Figure 6 The distance–time (a) and wave velocity – distance (b) diagrams for six successive shots with the FAMs of the same composition (empty signs — IPs 1 to 6; and filled signs — PSs 1 to 6); a stoichiometric hydrogen–air mixture

fore, in the example under consideration, the (averaged over 6 successive shots) DDT run-up distance L_{DDT} measured from the ignition source is $L_{\mathrm{DDT}} = 1.85 \pm 0.02$ m. Note that the transition from subsonic to supersonic flame propagation in the FAMs occurs between sections **1** and **2** where the flame accelerates sharply from 290–340 up to 1100–1360 m/s. Thereafter, the flame continues accelerating in sections **2** and **3** reaching a velocity $D_* = 1600$–1760 m/s which remains constant up to section 5. It is interesting that between sections **1** and **2**, the velocity of the combustion wave reaches the speed of sound in the combustion products of FAM. Considering that measuring sections **1**–**3** are located in the first section of the SDT with the Shchelkin spiral and the speed D_* is supersonic and constant from shot to shot, the combustion wave under consideration can also be interpreted as self-sustaining but nonideal detonation (in terminology of [17]) or quasi-detonation (in terminology of [2]) rather than normal detonation. In this case, the DDT run-up distance is somewhat between sections **2** and **3**, i. e., $L_{\mathrm{DDT}} \approx 0.6$ m.

Another parameter which allows determining the relative detonability of the FAM is the DDT run-up time t_{DDT}, i. e., the time interval from the instant of ignition to the instant of detonation onset. In the shots considered in Figs. 5 and 6, $t_{\mathrm{DDT}} = 2.98 \pm 0.02$ ms (averaged over 6 successive shots) if the condition $D \approx D_{\mathrm{CJ}}$ is adopted as a criterion for DDT, or $t_{\mathrm{DDT}} \approx 2.2$ ms if the condition $D \approx D_*$ is adopted as a criterion for DDT. The DDT run-up time is more sensitive to the properties of the FAM and is easier to measure with high accuracy (better than 3%) than the DDT run-up distance. In our opinion, for a comparative assessment of the detonability of FAMs that are close in their reaction and energy characteristics, it is the DDT run-up time that should be used as a measure of detonability provided the DDT run-up distance changes insignificantly.

For the tests with nonpremixed gases, the key data are the mass flow rates of FAM components. They are determined as follows. The mass flow rate of air is determined by the change in pressure in the air cylinder. The volume of air cylinder (430 l) is selected so that, on the one hand, a change in pressure during a test does not significantly affect the mass flow rate of air and, on the other hand, a change in pressure is sufficient to accurately determine the mass flow rate of air. At a constant mass flow rate of a combustible gas, such an approach

allows tracking the quality of FAM from shot to shot. For example, when the initial overpressure of air in the air cylinder is 0.27 MPa and the flow rate is 3 l/s, the change in the mass of air in the cylinder for a characteristic time of test does not exceed 20%.

The average mass flow rate of air during one test is calculated based on the measured pressure difference in the air cylinder before and after experiment, ΔP, the measured time Δt of air delivery into the SDT (time during which the air valve is open), and the cylinder volume V_r:

$$Q_{m,a} = \rho_0 \frac{V_r}{P_0} \frac{\Delta P}{\Delta t}$$

where ρ_0 and P_0 are the density and pressure of air at normal conditions (1.2 kg/m^3 and 101325 Pa, respectively). The pressure difference, ΔP, is determined based on the initial pressure in the cylinder before the test, $P_{r,0}$, and the pressure in the cylinder after the test, $P_{r,1}$, measured in a time interval of 5 min allocated to temperature compensation in the cylinder.

The mass flow rate of combustible gas is estimated by the time of complete decomposition of a sample of solid fuel. It is assumed that the total mass of combustible gas, m_f, is equal to $m_f = m_{f,0}k$ where $m_{f,0}$ is the mass of the sample, $k = 1 - x_r$ is the coefficient of fuel gasification, and x_r is the mass fraction of the solid residue. Then, the mass flow rate of fuel, $Q_{m,f}$, can be estimated by the formula:

$$Q_{m,f} = \frac{m_{f,0}}{\Delta t_f} (1 - x_r)$$

where Δt_f is the time of sample pyrolysis determined by the pressure curve at the level of 50% with respect to the maximum value. For example, for the decomposition temperature of 700 °C, $Q_{m,f} = 0.2$ g/s.

The mass flow rates of air and combustible gas are then used to determine the air-to-fuel mass ratio L_0. Recall that for FAMs based on heavy hydrocarbons such as aviation kerosene, the stoichiometric air-to-fuel mass ratio is approximately equal to $L_{0,\mathrm{st}} \approx 15$. Knowing the decomposition temperature T_d, the initial air temperature $T_a \approx 20$ °C, and the stoichiometric air-to-fuel mass ratio $L_{0,\mathrm{st}}$, one can estimate the temperature T_m of the FAM at the entrance to the SDT as

$$T_m \approx \frac{T_d + L_0 T_a}{1 + L_0} .$$

Since there is no provision of controlling the mass flow rate of the combustible gas expelling from the GG during the test with a non-premixed FAM, parameters of air supply are not stabilized. However, since the pressure change in the air cylinder during the experiment does not exceed 20%, the mass flow rate of air during the experiment (80–120 s) changes only slightly. As for the mass flow rate of the combustible gas, it varies in a wide range proportionally to the over-pressure in the GG. Therefore, such an approach makes it possible to change FAM composition from shot to shot in one test.

6 Experimental Results for Premixed Fuel–Air Mixtires and Discussion

Experiments with premixed gases are performed with FAMs based on hydrogen, acetylene, ethylene, propylene, propane–butane blend, n-pentane, and NG. In the experiments, technical gases are used without preliminary purification. Hydrogen of technical grade A (99.99%) is used. Acetylene is taken from a cylinder filled with acetone into a small sample tank at a temperature not exceeding -6 °C and then used to compose the FAM. Ethylene and propylene of technical grade intended for polymer synthesis are used.

A propane–butane blend is the propane–butane automobile (PBA) liquefied petroleum summer gas (propane-to-butane ratio is 50%/50% by weight). Pure pentane for analysis with the mass fraction of n-pentane of 98.5% is used. Natural gas containing 94.8% of methane is used.

In hydrogen FAMs, the volume content of hydrogen varies from 11% to 70% (the fuel-to-air equivalence ratio $\phi = 0.29$–5.56). In acetylene FAMs, the volume content of acetylene varies from 2.97% ($\phi = 0.36$) to 16.9% ($\phi = 2.42$) (richer acetylene–air mixtures are not studied herein due to the high soot formation). The volume content of ethylene in ethylene FAMs varies from 3.8% ($\phi = 0.56$) to 13% ($\phi = 2.13$). In propylene FAMs, the volume content of propylene varies from 3.0% ($\phi = 0.66$) to 6.5% ($\phi = 1.49$). In the PBA FAMs, the volume content of propane–butane varies from 2.6% ($\phi = 0.71$) to 5.1% ($\phi = 1.45$). In n-pentane FAMs, the volume content of n-pentane varies from 1.7% ($\phi = 0.66$) to 3.7% ($\phi = 1.46$). In the

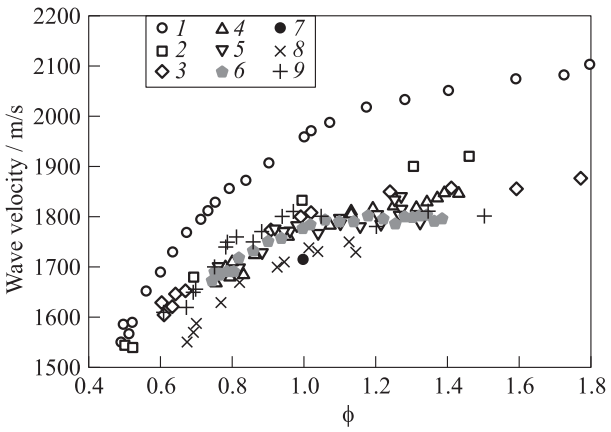

Figure 7 Measured dependences of the average detonation velocity in the measuring section of the SDT on the fuel-to-air equivalence ratio ϕ for FAMs based on hydrogen H_2 (*1*), acetylene C_2H_2 (*2*), ethylene C_2H_4 (*3*), propylene C_3H_6 (*4*), propane-butane C_3H_8–C_4H_{10} (*5*), *n*-pentane C_5H_{12} (*6*), NG (*7*), PP (*8*), and PE (*9*)

NG-based FAMs, the volume content of fuel varies from 7.75% ($\phi = 0.8$) to 11.2% ($\phi = 1.2$).

The experimental data are summarized in Fig. 7 showing the measured dependences of the average detonation velocity in the measuring section of the SDT on the fuel-to-air equivalence ratio ϕ in premixed and nonpremixed FAMs of various combustible gases. Each point is the result of averaging over at least 5–6 shots. In most of cases, the standard deviation does not exceed the maximum error in determining the wave velocity (3%), i. e., the maximum absolute error is ~ 60 m/s. In experiments with NG, detonation is detected only at a stoichiometric concentration of fuel (9.5 %(vol.)). The average velocity of the detonation wave is $D \approx 1700$ m/s, i. e., the relative velocity deficit is $(D_{CJ} - D)/D_{CJ} \approx 6\%$. In NG-based FAMs of compositions other than stoichiometric, low-velocity explosion processes are registered propagating at a velocity of 1200–1350 m/s.

Consideration of Fig. 7 allows one to draw the following general conclusions. First, in all cases when self-sustaining detonation is registered in the measuring section of the SDT, the average velocity of

the detonation wave is usually slightly lower than the calculated D_{CJ} value but very close to D_{CJ}. A small deficit in the detonation velocity is associated with the loss of momentum and energy on the smooth walls of the SDT [18]. Second, in these cases, DDT always (with some exceptions for FAMs at fuel-lean and fuel-rich limits) occurs inside the helical section of the SDT, i. e., $L_{\mathrm{DDT}} \approx 2$ m. Third, for all FAMs, there exists a minimum concentration of fuel at which there is no detonation in the measuring section of the SDT. Fourth, for all FAMs (except for acetylene FAMs, see above), there is a maximum fuel concentration at which there is no detonation in the measuring section of the SDT, either. The indicated minimum and maximum fuel concentrations in FAMs can be conditionally interpreted as the lower and upper concentration limits of DDT in the SDT of a given configuration. As for acetylene FAMs, according to the published data [19], the upper concentration limit of their detonation at normal pressure is close to 50% ($\phi = 11.9$). Fifth, at the lower and upper concentration limits, the average detonation velocity is approximately 3% to 5% lower than the Chapman–Jouguet velocity, D_{CJ}, and detonation propagates in the spinning mode. Sixth, the velocity of detonation wave inside the Shchelkin spiral is always lower than D_{CJ} (more than by 10%), which is associated with the elevated momentum and energy losses in the first section of the SDT containing obstacles in the form of wire coils. Note that replacement of Spiral 1 with BR = 0.46 by Spiral 2 with BR = 0.24 leads to a decrease in the relative deficit of the detonation velocity but does not change the results in principle. The specific features of the propagation of combustion waves in tubes with obstacles have been described in the literature many times and in detail (see, for example, [2, 17]) and, therefore, are not discussed here. It is also worth noting that the use of the standard spark plug ignition instead of the pulsed jet ignition in the SDT leads to considerable slowdown of the DDT process (approximately by a factor of 2).

Following Fig. 7, the detonation velocity at the lower concentration limit is ~ 1550 m/s for hydrogen and acetylene ($\phi = 0.49$–0.50), ~ 1630 m/s for ethylene ($\phi = 0.60$–0.61), ~ 1670 m/s for propylene ($\phi = 0.74$–0.75), and n-pentane ($\phi = 0.73$–0.74). In propane–butane FAMs with a fuel concentration of 2.7% ($\phi = 0.76$), the detonation velocity is 1700 m/s and at a concentration of 2.6% ($\phi = 0.71$),

detonation does not occur. Of all the studied premixed FAMs, the widest concentration limits of detonation in the SDT are inherent in the hydrogen-based FAMs and the narrowest ones are inherent in the NG-based FAMs. The maximum difference in the values of the detonation velocity between hydrogen and hydrocarbon FAMs is $\sim 15\%$. In the range $0.5 < \phi < 1.5$, the measured detonation velocities for FAMs based on acetylene, ethylene, propylene, propane-butane, and n-pentane differ insignificantly (less than by 6%).

The most interesting result is presented in Fig. 8 which shows the dependences of the measured DDT run-up time t_{DDT} on the fuel-to-air equivalence ratio ϕ in premixed and nonpremixed FAMs of different combustible gases (different curves and symbols correspond to different combustible gases). As noted above, in some experiments with hydrogen and acetylene, DDT occurs inside the Shchelkin spiral. In these experiments, t_{DDT} is taken as the time at which the condition $D \approx D_*$ is fulfilled. The absolute value of the DDT run-up time varies from ~ 2 to 35 ms, i. e., ~ 18 times. All $t_{\mathrm{DDT}}(\phi)$ curves are U-shaped with the pronounced minima for compositions slightly enriched in fuel ($\phi = 1.1$–1.4). The "tails" of the U-shaped curves sharply go upward

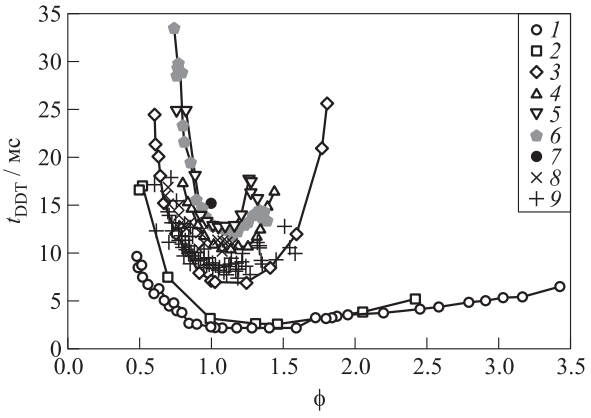

Figure 8 Dependences of the measured DDT run-up time t_{DDT} on the fuel-to-air equivalence ratio ϕ in FAMs of various combustible gases: hydrogen (*1*), acetylene (*2*), ethylene (*3*), propylene (*4*), propane-butane (*5*), n-pentane (*6*), NG (*7*), PP (*8*), and PE (*9*)

at the concentration limits of DDT, especially at the lower limit. In this case, the curves located above are embedded in the curves located below, i. e., for the upper curves, the boundaries of the existence of detonation are narrower than for the lower ones. For any given ϕ, hydrogen FAMs possess the shortest measured DDT run-up time and NG-based FAMs possess the longest DDT run-up time.

The data in Fig. 8 can be used directly for a comparative assessment of the detonability of different premixed FAMs using the DDT run-up time t_{DDT} as a detonability measure. For example, let us take a stoichiometric hydrogen–air mixture with $t_{\mathrm{DDT}} \approx 2.5$ ms as a reference FAM. Then, it can be argued that all hydrogen FAMs with $0.9 < \phi < 1.6$ have the same detonability as the reference FAM. In addition, acetylene-based FAMs with $1 < \phi < 1.7$ have the same detonability. If one takes into account that the detonation velocities in the indicated mixtures differ insignificantly (less than by 10%, see Fig. 7), this means that the reference FAM can be used for predictive physical modeling of explosion processes involving the indicated "equivalent" mixtures. Another example of "equivalent" FAMs: propane–butane FAM with $1 < \phi < 1.2$, propylene FAMs with $\phi = 0.9$ and 1.3, and ethylene FAMs with $\phi = 0.8$ and 1.6.

According to Fig. 8, one can rank premixed FAMs in descending order of their detonability under the same conditions as follows: $H_2 > C_2H_2 > C_2H_4 > C_3H_6 > C_5H_{12} > C_3H_8 + C_4H_{10}(\mathrm{PBA}) > CH_4$. It is interesting that FAMs based on n-pentane turn out to possess somewhat higher detonability than FAMs based on propane-butane blend which is not consistent with the ranking of FAM detonability in terms of the average cell size of multifront detonation [2]. Apparently, the difference in obtaining a detonation via DDT and via direct initiation manifests itself: in DDT, the main role is played by low-temperature self-ignition of FAM behind a relatively weak shock wave, whereas in the direct initiation of detonation, the high-temperature self-ignition of FAM behind a strong shock wave is of primary importance. With an increase in the number of carbon atoms in the alkane molecule, the low-temperature self-ignition delay in the region of the negative temperature coefficient of the reaction rate is known to decrease [20]. This means that the heavier alkane hydrocarbons should exhibit higher detonability in terms of the DDT run-up time than the lighter ones and the ranking shown above confirms this implication.

7 Experimental Results for Nonpremixed Fuel–Air Mixtures and Discussion

The tests with nonpremixed FAMs are first performed with FAMs based on the propane-butane blend and NG to debug the methodology and to obtain comparative data with premixed FAMs. Other gaseous fuels (hydrogen, acetylene, propane, propylene, etc.) are also tested in the nonpremixed mode but the corresponding results are not discussed herein.

In experiments with the nonpremixed FAMs based on propane-butane and NG with the overall stoichiometric composition, DDT is also obtained at $L_{\mathrm{DDT}} \approx 2$ m. The corresponding DDT run-up time t_{DDT} is 13 and 15 ms. The values of t_{DDT} are seen to be very similar to those registered for the corresponding premixed FAMs (see Fig. 8). Moreover, an unstable limiting (spinning) detonation mode is registered in the NG–air mixture with detonation decay in the measuring section.

Detonability of nonpremixed FAMs based on PP and PE pyrolysis products at decomposition temperatures on the level of 800 °C were also studied. Figures 7 and 8 show the corresponding dependences of the detonation velocity and t_{DDT} on the fuel-to-air equivalence ratio. As seen, the nonpremixed FAM based on the PP pyrolysis products exhibits higher detonability than the premixed propylene-based FAM, whereas the nonpremixed FAM based on the PE pyrolysis products exhibits detonability comparable with the premixed ethylene-based FAM. The possible reason for the enhancement of FAM detonability with the decomposition temperature is the increase in the content of light hydrocarbons (mostly, hydrogen and ethylene) in PP pyrolysis products.

8 Concluding Remarks

Thus, we propose a new method for determining the relative detonability of fuels based on measured values of the DDT run-up distance and/or time in the SDT. Using this method, we rank various premixed and nonpremixed FAMs by their detonability under substantially identical thermodynamic and gasdynamic conditions. In the experiments, premixed and nonpremixed FAMs based on hydro-

gen, acetylene, ethylene, propylene, propane-butane, n-pentane, NG, and gaseous pyrolysis products of PP and PE of various compositions are used: from extremely fuel-lean to extremely fuel-rich at normal pressure.

In all experiments in which self-sustaining detonation is registered in the measuring section of the SDT, DDT mostly occurs inside the helical section of the SDT. The minimum and maximum fuel concentrations in FAMs are determined at which detonation does not occur in the measuring section of the SDT. The indicated minimum and maximum concentrations of fuels are proposed to be conditionally interpreted as the lower and upper concentration limits of DDT in the SDT of a given configuration. At the lower and upper concentration limits, the average detonation velocity is lower by about 3%–5% than the CJ velocity, D_{CJ}. The velocity of the detonation wave at the exit from the Shchelkin spiral is always lower than D_{CJ} (more than by 10%). Of all the studied FAMs, the widest concentration limits of DDT in the SDT are inherent in hydrogen-based FAMs and the narrowest concentration limits of DDT in the SDT are inherent in the NG-based FAMs. The maximum difference in the values of the detonation velocity between hydrogen and hydrocarbon FAMs is $\sim 15\%$. In the range of the fuel-to-air equivalence ratio $0.5 < \phi < 1.5$, the measured detonation velocities for FAMs based on acetylene, ethylene, propylene, propane-butane, and n-pentane differ insignificantly (no more than by 6%).

For all the FAMs studied, the absolute value of the DDT run-up time t_{DDT} varies from ~ 2 to ~ 35 ms. All $t_{\mathrm{DDT}}(\phi)$ curves have an U-shape with the pronounced minima for compositions enriched in fuel ($\phi = 1.1$–1.4). The "tails" of the U-shaped curves sharply go upward at the concentration limits of DDT, especially at the lower limit. In this case, the curves located above are embedded in the curves located below, i. e., for the upper curves, the boundaries of the existence of DDT are narrower than for the lower ones. For any given ϕ, hydrogen-based FAMs possess the shortest measured DDT run-up time, and NG-based FAMs exhibit the longest DDT run-up time. In general, the tests with nonpremixed FAMs show the results similar to those obtained for premixed FAMs.

Tests on the DDT in nonpremixed mixtures of hot PP and PE pyrolysis products with air are performed. It is shown that in the FAMs

somewhat enriched in fuel ($\phi = 1.1$–1.4) at normal pressure and elevated initial temperature (60–90 °C), the products of PP and PE pyrolysis exhibit detonability close to that of the premixed stoichiometric propylene–air and ethylene–air mixtures at normal conditions, respectively. Detonability of PP and PE pyrolysis products increases with the decomposition temperature. The measured detonation velocities in the FAMs based on the PP and PE pyrolysis products are on the level of 1700–1800 m/s, i. e., the exothermicity of the PP and PE pyrolysis products in air is close to that of jet propulsion fuels.

The data obtained are used for a comparative assessment of the detonability of different FAMs, using the DDT run-up time t_{DDT} as a detonability measure. All the FAMs considered are ranked in the descending order of detonability:

$$\begin{aligned} \mathrm{H_2} > \mathrm{C_2H_2} > \mathrm{C_2H_4} > \mathrm{PE}\,(T_d = 800\ ^\circ\mathrm{C}) > \mathrm{PP}\,(T_d = 800\ ^\circ\mathrm{C}) \\ > \mathrm{C_3H_6} > n\text{-}\mathrm{C_5H_{12}} > \mathrm{C_3H_8} + \mathrm{C_4H_{10}(PBA)} > \mathrm{CH_4(NG)}\,. \end{aligned}$$

At $T_d = 800$ °C, the nonpremixed FAMs based on the PE and PP pyrolysis products exhibit higher detonability than the premixed ethylene-based and propylene-based FAMs, respectively. The FAMs based on n-pentane possess somewhat higher detonability than the FAMs based on propane-butane blend, which is apparently due to the difference in obtaining a detonation via DDT and via direct initiation: in DDT, the main role is played by the low-temperature self-ignition of FAM behind a relatively weak shock wave, whereas in the direct initiation of detonation, the high-temperature self-ignition of FAM behind a strong shock wave is of primary importance.

In view of the relatively high detonability of PE and PP pyrolysis products in air, one can consider feasible the use of gasification/pyrolysis products of SCMs like PE and PP in solid-fuel ramjets operating on detonation. Chromatographic analysis of gaseous pyrolysis products of PE and PP at decomposition temperatures ranging from 650 to 850 °C shows they mainly consist of light hydrocarbons and hydrogen. At the highest studied decomposition temperatures, the content of hydrogen is also getting large ($\sim 2\,\%$(wt.)).

The concept of "equivalent" FAMs having the same or similar detonability under the same conditions is proposed. "Equivalent" FAMs can be used for predictive physical modeling of explosion processes

involving FAMs of other fuels. The ranking of FAMs in terms of their relative detonability shown above allows choosing the ethylene- and propylene-based FAMs for physical modeling of the operation process in the PE- and PP-fueled solid-fuel ramjets.

Finally, one important issue must be addressed. In view that the DDT process is known to be geometry dependent, does it mean that the proposed ranking is apparatus dependent and any changes in the SDT geometry and scale may result in different ranking of FAMs? On the one hand, to partly answer to this question, we have studied the sensitivity of the results to the SDT configuration by changing the blockage ratio of the Shchelkin spiral in the flame acceleration section of the SDT for hydrogen-, ethylene-, and propylene-based FAMs. All main (qualitative) conclusions are confirmed by this sensitivity study. On the other hand, other methods for estimating explosibility/detonability of FAMs are apparatus dependent, e. g., the detonability limits are known to depend on the detonation tube diameter but this fact does not reduce the value of detected trends. Anyway, further research is needed to better understand this issue.

Acknowledgments

This work is partly performed due to the subsidies allocated by the N. N. Semenov Federal Research Center for Chemical Physics of the Russian Academy of Sciences for the implementation of the State Task No. 0082-2019-0006 (State registration number AAAA-A21-121011990037-8) and by the Federal State Institution "Scientific Research Institute of System Analysis of the Russian Academy of Sciences" to implement the state assignment on the topic No. 0580-2021-0005.

References

1. Kasahara, J., and S. Frolov. 2015. Present status of pulse and rotating detonation engine research. *25th Colloquium (International) on the Dynamics of Explosions and Reactive Systems*. Leads, U.K. Paper 304.
2. Lee, J. H. S. 2008. *The detonation phenomenon*. New York, NY: The Cambridge University Press. Available at: www.cambridge.org/9780521897235 (accessed January 10, 2021).

3. Frolov, S. M., and B. E. Gel'fand. 1990. On the limiting diameter for propagation of gas detonation in tubes. *Dokl. Akad. Nauk SSSR* 312(5):1177–1180.
4. Sokolik, A. S., and K. I. Shchelkin. 1933. Rasprostranenie plameni v smesyakh metana s kislorodom v zakrytykh trubkakh [Flame propagation in mixtures of metane with oxygen in closed tubes]. *Zh. Fiz. Khimii* 4(1):109–128.
5. Sokolik, A. S., and K. I. Shchelkin. 1933. Detonatsionnaya sposobnost' kislorodnykh smesey uglevodorodov zhirnogo ryada i aromaticheskikh [Detonability of oxygen mixtures of saturated and aromatic hydrocarbons]. *Zh. Fiz. Khimii* 4(2):129–131.
6. Shchelkin, K. I. 1940. Vliyanie sherokhovatosti truby na vozniknovenie i rasprostranenie detonatsii v gazakh [Effect of tube roughness on the onset and propagation of detonation in gases]. *Zh. Exp. Teor. Fiz.* 10(7):823–827.
7. Papavassiliou, J., A. Makris, R. Knystautas, J. H. S. Lee, C. K. Westbrook, and W. J. Pitz. 1993. Measurements of cellular structure in spray detonations. *Dynamics aspects of explosion phenomena*. Eds. A. L. Kuhl, J.-C. Leyer, A. A. Borisov, and W. A. Sirignano. Progress in astronautics and aeronautics ser. Washington, D.C.: AIAA Inc. 154:148–169.
8. Frolov, S. M. 2006. Liquid-fueled air-breathing pulse detonation engine demonstrator: Operation principles and performance. *J. Propul. Power* 6:1162–1169. doi: 10.2514/1.17968.
9. Frolov, S. M., V. I. Zvegintsev, V. S. Aksenov, I. V. Bilera, V. V. Kazachenko, I. O. Shamshin, P. A. Gusev, M. S. Belotserkovskaya, and E. V. Koverzanova. 2018. Detonatsionnaya sposobnost' vozdushnykh smesey produktov piroliza polipropilena [Detonability of air mixtures of the polypropylene pyrolysis products]. *Goren. Vzryv (Mosk.) — Combustion and Explosion* 11(4):44–60. doi: 10.30826/CE18110406.
10. Frolov, S. M., V. I. Zvegintsev, V. S. Aksenov, I. V. Bilera, V. V. Kazachenko, I. O. Shamshin, P. A. Gusev, and M. S. Belotserkovskaya. 2019. Deflagration-to-detonation transition in the air mixtures of polypropylene pyrolysis products. *Dokl. Phys. Chem.* 488(1):129–133. doi: 10.1134/S0012501619090045.
11. Voinov, A. N. 1957. Investigation into detonation and self-ignition in reciprocating engines operating on light fuel. Moscow: Institute of Chemical Physics of the USSR Academy of Sciences. DSc Thesis.
12. Hensinger, D. M., J. A. Masson, K. Hom, and A. K. Oppenheim. 1992. Jet-plume injection and combustion. SAE Paper No. 920414.

13. Frolov, S. M. 2006. Initiation of strong reactive shocks and detonation by traveling ignition pulses. *J. Loss Prevent. Proc.* 19(2-3):238–244. doi: 10.1016/j.jlp.2005.04.006.
14. Frolov, S. M., V. S. Aksenov, A. V. Dubrovskii, A. E. Zangiev, V. S. Ivanov, S. N. Medvedev, and I. O. Shamshin. 2015. Chemiionization and acoustic diagnostics of the process in continuous- and pulse-detonation combustors. *Dokl. Phys. Chem.* 465(1):273–27. doi: 10.1134/S0012501615110019.
15. Borisov, A. A., B. E. Gelfand, S. A. Loban', A. E. Mailkov, and S. V. Khomik. 1982. Issledovanie predelov detonatsii toplivovozdushnykh smesey v gladkikh i sherokhovatykh trubakh [Study of detonation limits in fuel–air mixtures in smooth and rough tubes]. *Khim. Fizika* 1(6):848–853.
16. Zvegintsev, V. I., A. V. Fedorychev, D. V. Zhesterev, I. R. Mishkin, and S. M. Frolov. 2019. Gazifikatsiya legkoplavkikh uglevodorodnykh materialov v vysokotemperaturnom gazovom potoke [Gasification of low-melting hydrocarbon materials in high-temperature gas flow]. *Goren. Vzryv (Mosk.) — Combustion and Explosion* 12(3):108–116.
17. Zel'dovich, Ya. B., A. A. Borisov, B. E. Gel'fand, S. M. Frolov, and A. E. Mailkov. 1988. Nonideal detonation waves in rough tubes. *Dynamics of explosions*. Eds. A. L. Kuhl, J. R. Bowen, J.-C. Leyer, and A. A. Borisov. Progress in astronautics and aeronautics ser. Washington, D.C.: AIAA Inc. 114:211–231.
18. Zel'dovich, Ya. B., and A. S. Kompaneets. 1955. *Teoriya detonatsii* [The theory of detonation]. Moscow: Gostekhteorizdat. 268 p.
19. Antonov, V. N., and A. S. Lapidis. 1970. *Proizvodstvo atsetilena* [Production of acetylene]. Moscow: Khimiya Publs. 415 p.
20. Basevich, V. Ya., A. A. Belyaev, V. S. Posvyanskii, and S. M. Frolov. 2013. Mechanisms of the oxidation and combustion of normal paraffin hydrocarbons: Transition from C_1–C_{10} to C_{11}–C_{16}. *Rus. J. Phys. Chem. B.* 7(2):161–169. doi: 10.1134/S1990793113020103.